How molar ratio between two anions affects physicochemical properties and biological activity of double salt ionic liquids (DSILs)?

Tomasz Rzemieniecki,[a],* Damian K. Kaczmarek,[a] Witold Stachowiak,[a] Katarzyna Marcinkowska,[b] Michał Niemczak[a]

[a] Faculty of Chemical Technology, Poznan University of Technology, ul. Berdychowo 4, Poznan 60-965, Poland

[b] Department of Weed Science and Plant Protection Techniques, Institute of Plant Protection–National Research Institute, Poznan 60-318, Poland

* Tomasz Rzemieniecki: Faculty of Chemical Technology, Poznan University of Technology, ul. Berdychowo 4, Poznan 60-965, Poland

E-mail address: tomasz.rzemieniecki@put.poznan.pl

Tel. +48 61 665 3681

1

Abstract:

The strategy of mixing ionic liquids opens up new possibilities for obtaining liquid chemical systems (*i.e.*, double salt ionic liquids, DSILs) with well-defined, beneficial properties, which is particularly important for the design of new biologically active substances. Here, we describe the application of the DSIL strategy for obtaining new systems containing a common amphiphilic cation with a hexadecyl substituent and 2 anions derived from synthetic auxins at the different molar ratio – MCPA and dicamba, both suitable for use as novel herbicides with enhanced efficiency. Detailed analysis of the NMR spectra indicates the presence of new interactions in the structure of DSILs, which affect the chemical environment of the ions and are strictly dependent on the molar ratio of the parent ionic liquids. Moreover, a non-additive effect of combining two surface-inactive anions on the surface activity of DSILs was discovered. DSILs with molar ratios from 8:2 to 2:8 had better surface activity compared to their starting components containing only one anion. Moreover, in greenhouse experiments DSIL containing molar fraction of dicamba equal to 0.2 showed significantly better efficiency than the other tested systems. This enhancement can be explained by the occurrence of a synergistic effect between both utilized anions. However, insertion into DSIL greater content of the dicamba anion nullified this beneficial effect. The initial ecotoxicity studies also pointed out potential risks associated with the increased toxicity of the new DSIL systems to non-target organisms, which warrants further research on the effects of mixing ionic liquids on environmental loading.

Keywords: *ionic liquid mixtures*, *surface active agents*, *spectral analysis*, *herbicides*, *aquatic toxicity*, *weeds*

1. Introduction

The concept of ionic liquids (ILs) has evolved significantly over the past 40 years. The considerable amount of data obtained from the studies of compounds belonging to this group and the property models created from them have made it possible to verify early generalizations about ILs, that they were supposedly safe, non-toxic, thermally stable and "green" compounds, particularly in comparison to conventional organic solvents.[1] When the potential problems of recycling and disposal of ILs were taken into account, as well as the effects of their introduction into the environment, the search for new sources of ILs ions, and safer methods of their synthesis became important.[2–4]

However, the possibility of almost free[5] adaptation of ILs' structure to the desired properties (so-called "designability") – including in the context of their toxicity – and the related multiplicity of their potential applications in various industries remains an unquestionable advantage. As a result of the development of specific models on the basis of collected experimental data, methods based on machine learning[6–8] are now becoming helpful in achieving favorable results and predicting the properties of designed ILs. However, the desired effect can be achieved not only by selecting the right combination of cation and anion or by slight structural modifications to one of the ions (*e.g.*, altering the length of an alkyl chain), but also by creating entirely new ionic systems as a result of mixing 2 or more ILs. Such an approach offers an additional degree of freedom in the choice of cation and anion,[9] does not require the design of a new synthesis process (as in the case of anion exchange or other structural modifications), and the resulting IL mixtures with potentially non-ideal characteristics can have new and unique properties that none of the constituent ionic liquids possess.[10,11] To distinguish such systems from simple mixtures, the name double salt ionic liquids (DSILs) has been proposed for them.[12] Analogous to deep eutectic solvents (DESs), numerous properties of DSILs result from chemical interactions between the constituent ions, and a change in the molar ratio of parent ILs can result in a significant change in the properties of a given system,[9] which justifies investigating the physical, physicochemical and biological properties of various DSIL systems. Moreover, in some cases DSILs can become the basis for new DESs.[1]

In view of the advantages offered by the liquid, modular form of the active ingredient, including the ability to avoid the problems associated with the use of a solid form of the active ingredient (*e.g.*, low bioavailability, polymorphism) and at the same time increase activity against the target organism through structural modifications or the use of an appropriate combination of

3

ions, adherence to ILs (and, more recently, DESs[13,14]) concept is a legitimate strategy for designing new biologically active substances.[15–18] In agrochemical treatments, it is popular to use more than one herbicide, since such a measure broadens the spectrum of action of the herbicide formulation, and can also counteract the acquisition of resistance by undesirable vegetation.[19,20] It is also known that the transformation of the herbicide active ingredient into an IL may result in a significant increase in the biological activity of the new substance against weeds compared to reference formulations.[21] At the same time, it should be emphasized that the observed increase in efficacy is mainly due to the favorable surface properties of the IL solution applied, which improves the penetration and action of the herbicide anion.[22] Thus, it becomes reasonable to use a DSIL strategy and combine the surface-active cation with two or more active anions originating from known herbicides (e.g., 4-chloro-2-methylphenoxyacetic acid (MCPA) or 3,6-dichloro-2-methoxybenzoic acid (dicamba)).

Given that the properties of DSILs are strictly dependent on the molar ratio between constituents, in this study we have attempted to further elucidate the phenomenon of synergistic action for DSILs for agrochemical applications and to find the optimal molar ratio of the parent ILs which will provide the most favorable properties. We have also provided a detailed spectral and physicochemical characterization of the new DSILs as well as preliminary evaluation of their aqueous toxicity toward model freshwater algae – *Chlorella vulgaris*.

2. Experimental

2.1. Materials

2-[2-(Dimethylamino)ethoxy]ethanol (purity 98%) was purchased from Merck and additionally purified by vacuum rectification. The colorless fraction boiling at 79–80 °C at a pressure of 0.2 mbar was collected and used for further syntheses. 1-Bromohexadecane (purity 97%), anion exchange resin AmberTec™ UP550 OH, and activated carbon (powder – 100 mesh particle size), were purchased from Merck (Darmstadt, Germany) and used without further purification. Ethanol (purity ≥99.8%), methanol (purity ≥99.8%), 2-propanol (purity ≥98%), and acetonitrile (purity 99%) were obtained from Avantor (Gliwice, Poland) and used without further purification. (4-Chloro-2-methylphenoxy)acetic acid (MCPA, purity 94%) and 3,6-dichloro-2-methoxybenzoic acid (dicamba, purity 99%) used in this study were supplied by Pestinova (Jaworzno, Poland). In addition, MCPA was purified by recrystallization followed by treatment with activated carbon according to the previously described protocol.[23] Of the compounds to be used for OECD TG 201 medium preparation boric acid (purity ≥99.5%), potassium dihydrogen phosphate (purity ≥99.5%), sodium bicarbonate (purity ≥99.7%), copper(II)

4

chloride dihydrate (purity ≥99.0%), manganese(II) chloride tetrahydrate (purity ≥99.0%), zinc chloride (purity ≥99.0%), sodium molybdate dihydrate (purity ≥99.5%), and ethylenediaminetetraacetic acid disodium salt dihydrate (EDTA, purity ≥99.0%) were purchased from Merck (Darmstadt, Germany); ammonium chloride (purity ≥99.0%), magnesium chloride hexahydrate (purity ≥99.0%), calcium chloride dihydrate (purity ≥99.0%) were purchased from Th. Geyer Ingredients (Höxter-Stahle, Germany); magnesium sulfate(VI) heptahydrate (purity ≥99.0%) was purchased from Alfachem (Poznań, Poland); cobalt(II) chloride hexahydrate (purity ≥99.0%) and iron(III) chloride hexahydrate (purity ≥99.0%) were purchased from Pol-Aura (Morąg, Poland). Water for apparatus calibration, surface activity measurements and biological assay studies was deionized, with a conductivity <0.1 μS·cm^{-1}, from demineralizer HLP Smart 1000 (Hydrolab, Straszyn, Poland).

2.2. Methods

2.2.1. General

^{1}H NMR spectra were acquired using Varian VNMR-S 400 MHz spectrometer (Palo Alto, USA) with TMS as the internal standard, using deuterated dimethylsulfoxide (DMSO-d_6) as a solvent. Samples of 0.1 ±0.001 g were dissolved in 0.6 cm^3 of DMSO-d_6 to obtain comparable spectra. ^{13}C NMR spectra were obtained with the same instrument at 100 MHz. The FT-IR spectra were recorded on IFS 66v/S spectrometer (Bruker Optics, Ettlinger, Germany). The data were sampled from 4000 to 400 cm^{-1} and visualized using Spectragryph 1.2.13[24] software. The water content in all obtained products was measured with a TitroLine 7500 KF trace apparatus (SI Analytics, Germany) using the Karl Fischer titration method according to the previously described procedure.[22] Differential scanning calorimeter (DSC) was performed on DSC 209 F1 Phoenix unit (Netzsch, Germany. Samples between 5 and 20 mg were placed in platinum pans and were heated from 25 to 120 °C at a heating rate of 10 °C min^{-1} and cooled at a cooling rate of 10 °C min^{-1} to -80 °C. After that, samples were heated again to 120 °C and subsequently cooled to 25 °C.

2.2.2. Preparation of ILs

To obtain parent ILs with MCPA and dicamba anions, a quaternization of 2-[2-(dimethylamino)ethoxy]ethanol with 1-bromohexadecane in acetonitrile was conducted analogously to the previously described procedure[25] using a 100 cm^3 EasyMax reactor equipped with ReactIR$^®$ 15 spectrometer, a reflux condenser, a stir bar and a temperature sensor. The FT-IR spectra acquired *in situ* were subsequently normalized using Pearson's

5

correction on the entire dataset, and the optimal reaction time was established based on the change in relative absorbance of the band occurring at 919 cm^{-1}. The obtained hexadecyl[2-(2-hydroxyethoxy)ethyl]dimethylammonium bromide was then subjected to the two-step anion exchange reaction according to the previously described procedure.[26] In the first stage, 40 cm^3 of ethanolic solution of hexadecyl[2-(2-hydroxyethoxy)ethyl]dimethylammonium bromide (0.1 mol) was introduced into a suspension of 80 cm^3 of the AmberTec™ UP550 OH anionic resin in 100 cm^3 of ethanol. The mixture was stirred for 1 h at 25 °C, and in the next step, the resin was filtered and washed three times with small volumes (15 cm^3) of ethanol. The solution of hexadecyl[2-(2-hydroxyethoxy)ethyl]dimethylammonium hydroxide was subsequently neutralized with an equimolar amount of the herbicidal acid (MCPA or dicamba). The solvent was subsequently evaporated using a rotary evaporator. To remove the water formed during the neutralization step for analytical purposes, the ILs were subjected to two-step azeotropic distillation: first, they were dissolved in 20 cm^3 of 2-propanol and the 2-propanol-water binary azeotropewas distilled off before evaporating the excess of pure 2-propanol. To remove the residual 2-propanol, the ILs were additionally dissolved in 20 cm^3 of anhydrous methanol and subjected to another step of evaporation. Finally, the obtained ILs were dried under reduced pressure (5 mbar) at 75 °C for 48 h. Both synthesized ILs were stored under reduced pressure over P_4O_{10} to reduce water absorption.

2.2.3. Preparation of DSILs

A series of DSILs with varying molar fraction of dicamba anion was prepared by mixing the ethanolic solutions of single-ion ILs. First, 0.05 mol of each parent IL (weighed with the accuracy of ±0.0001 g) was dissolved in ethanol to obtain 50 cm^3 of solution, and then both solutions were combined in such volumes as to obtain DSILs with the following MCPA-dicamba molar ratios: 9:1, 8:2, 7:3, 6:4, 5:5, 4:6, 3:7, 2:8, and 1:9. To ensure full reproducibility of the results for all DSILs, the same single-anion ILs solutions of a well-defined concentration (1 ±10^{-5} mol dm^{-3}) were used to obtain the solutions, which were dispensed using the same pre-calibrated automatic pipette. The obtained mixtures were vigorously stirred for 5 min, and then the solvent was evaporated. The products were pre-dried under reduced pressure conditions (5 mbar, 75 °C) analogously as for single-anion ILs. For analytical purposes, a significant amount of water was removed from the obtained products by two-step azeotropic distillation. The obtained product was dissolved in 30 cm^3 of 2-propanol, after which the azeotrope and the remaining 2-propanol were evaporated under reduced pressure. The residue was dried using a Schlenk line (pressure: 2·10^{-5} bar) while heating to 65 °C for at least 6 hours. Subsequently, the

residual 2-propanol was removed by performing azeotropic distillation with methanol and drying the residue as in the previous step. The obtained DSILs were stored analogously as in the case of their parent ILs. After drying, using a dicamba-derived single-anion IL and a DSIL containing 0.9 molar fraction of dicamba anion, 2 additional DSILs with molar ratios of MCPA and dicamba anions of 5:95 and 1:99 were also obtained for additional spectral studies according to an analogous method.

2.2.4. Density

Density of DSILs was determined using an Automatic Density Meter DDM2911 (Rudolph Research Analytical, Hackettstown, NJ) equipped with a Peltier module for precise temperature control, with the mechanical oscillator method. The measurement was acquired at 20 °C in 5 repetitions for each of the samples (approximately $1.0 \, \text{cm}^3$). Before the series of measurements, the apparatus was subjected to a two-point calibration using deionized water and air as the references. After each series of measurements, the densimeter was washed with water and organic solvents (methanol and acetone) and dried with airflow. The uncertainty of the density measurement was estimated to be less than $5 \times 10^{-4} \, \text{g cm}^{-3}$. Based on the experimental density values obtained at 20 °C (ρ_{20}), and average molecular weights of ILs and DSILs (M_w), the following parameters were calculated: molar volume (V_m^{20}), excess molar volume (V^{E20}), average volume of a single ionic pair (V_{ip}^{20}), lattice energy (U_{POT}^{20}), and standard molar entropy ($S^{\circ 20}$), according to the equations below[27,28]:

$$V_m{}^{20} = \frac{M_w}{(N \cdot \rho_{20})} \tag{1}$$

$$V_m{}^{E20} = \frac{x_A M_{wA} + x_B M_{wB}}{\rho_{20AB}} - \frac{x_A M_{wA}}{\rho_{20A}} - \frac{x_B M_{wB}}{\rho_{20B}} \tag{2}$$

$$U_{POT}{}^{20} = 1981.2 \cdot \left(\frac{\rho_{20}}{M_w}\right)^{\frac{1}{3}} + 103.8 \tag{3}$$

$$S^{\circ 20} = 1246.5 \cdot V_m{}^{20} + 29.5 \tag{4}$$

In the eq.2, x corresponds to the molar fraction, M_w is molecular weight, and ρ_{20} is density value measured at 20 °C. Subscripts **A** and **B** refer to the parent ILs, and the subscript **AB** refers to their mixtures – DSILs.

2.2.5. Refractive index

Refractive index was determined by using an Automatic Refractometer J357 (Rudolph Research Analytical, Hackettstown, NJ) with electronic temperature control at 20 °C for all

7

DSILs. The apparatus was calibrated using deionized water before use, and the accuracy of refractive index measurements was $\pm\,2\times10^{-4}$ according to the manufacturer's specifications. Based on the experimental refractive index values obtained at 20 °C for parent ILs **A** and **B**, differences between the experimental values recorded for DSILs and the theoretical $n_D{}^{20}$ values was calculated according to the equation below:

$$\Delta n_D{}^{20} = n_{D\cdot AB}^{20} - (x_A n_{D\cdot A}^{20} + x_B n_{D\cdot B}^{20}) \tag{5}$$

where subscripts **A** and **B** refer to the parent ILs, and the subscript **AB** refers to the respective DSIL.

2.2.6. Surface activity

The surface tension and contact angle measurements were carried out using a DSA 100E analyzer (Krüss, Germany) at 25 °C. According to the manufacturer, the measurement accuracy of this instrument amounts to ±0.001 mN m^{-1}. The surface tension was determined using the drop shape method. Basically, the principle of this method is to form an axisymmetric drop at the tip of a needle of known diameter. The image of the drop is taken with a CCD camera and digitized. The surface tension (γ, mN m^{-1}) was calculated according to the results of the drop profile analysis according to the Laplace equation. The value of the surface tension and contact angle allowed for calculation of the CMC and surface tension at CMC (γ_{CMC}) based on the plot γ vs log C using a linear regression analysis method. The temperature was controlled using a Fisherbrand FBH604 thermostatic bath (Fisher, Germany, accuracy ±0.1 °C). The determination of the contact angle (CA) was based on the sessile drop method. The drops of solution are deposited on a solid hydrophobic surface (paraffin). The images of the drops were taken with a CCD camera, digitized and evaluated using Young-Laplace fitting. The CA was determined as the slope of the tangent line at the contact point between the 3 phases (solution, paraffin surface, and air). The measured error of the CA determination in this method is estimated to be less than 0.1° by the manufacturer.

2.2.7. Greenhouse experiments

Common lambsquarters (*Chenopodium album* L.) was used in greenhouse experiments as test plant during the evaluation of herbicidal efficacy of the obtained single-anion ILs and the selected DSILs, for which the value of the molar fraction of dicamba anion was 0.2, 0.4, 0.6 and 0.8. All plants were grown in 0.5 dm^3 plastic pots containing commercial peat-based potting material (Lasland, Grądy, Poland). Stable conditions (temperature of 20 ±2 °C, humidity of 60% and a photoperiod of 16/8 day/night hours) were maintained in the greenhouse during the

entire growth period. Within 10 days after emergence, the plants were thinned to 5 per pot and watered when necessary. The greenhouse experiments were performed in completely randomized design with 12 independent experimental units (6 ILs or DSILs and 6 reference herbicides). Each test was carried out in 3 replications. The plants were treated by herbicides at the 3–4 leaves growth stage (BBCH 13–14). Commercially available herbicide: Chwastox Extra 300 SL (300 g dm^{-3} of sodium and potassium salts of MCPA, CIECH Sarzyna, Poland, equivalent to 10.02 mmol dm^{-3}) was used as a reference product for MCPA-based single-anion IL. For the single-anion IL involving dicamba, Dicash 480 SL (480 g dm^{-3} dicamba as dimethylamine salt, Sharda Europe, Dilbeek, Belgium, equivalent to 4.54 mmol dm^{-3}) was used as a reference instead. The obtained single-anion ILs and their reference herbicides were applied in doses corresponding to 400 g ha^{-1} of the active ingredient (a.i.) for MCPA-based herbicides and 200 g ha^{-1} of the active ingredient (a.i.) for dicamba-based herbicides.

Non-standard doses for the 4 tested DSILs with varying molar fraction of dicamba anion were used to capture differences between the experimental objects. The total doses of the DSILs were determined via interpolation. The following doses were used as input data:

- 400 g ha^{-1} (MCPA only, $w_{dic} = 0$),
- 340 g ha^{-1} (standard MCPA-dicamba mix Chwastox Turbo 340 SL,[25] $w_{dic} = 0.118$),
- 200 g ha^{-1} (dicamba only, $w_{dic} = 1$).

Where w_{dic} is mass fraction of dicamba anion.

To ensure that the determined function did not take values less than 200 g ha^{-1}, an additional input was taken: 205 g ha^{-1} for $w_{dic} = 0.8$. Based on the 4 points described above, a polynomial function of 3rd degree was determined (Fig. 1a):

$$D_{total} = -194.30\, w_{dic}{}^3 + 568.50\, w_{dic}{}^2 - 574.19\, w_{dic} + 400.00 \tag{6}$$

Where D_{total} is total dose of both MCPA and dicamba anions (g ha^{-1}) for a given w_{dic} value. Based on the determined function, the D_{total} values for the tested DSILs were found and rounded off. The dependence of the D_{total}, D_{MCPA} (MCPA anion dose) and D_{dic} (dicamba anion dose) on the w_{dic} is shown in Fig. 1b. The exact dose values and regression parameters for the found functions are provided in Supplementary Data (Tables A.1 and A.2).

9
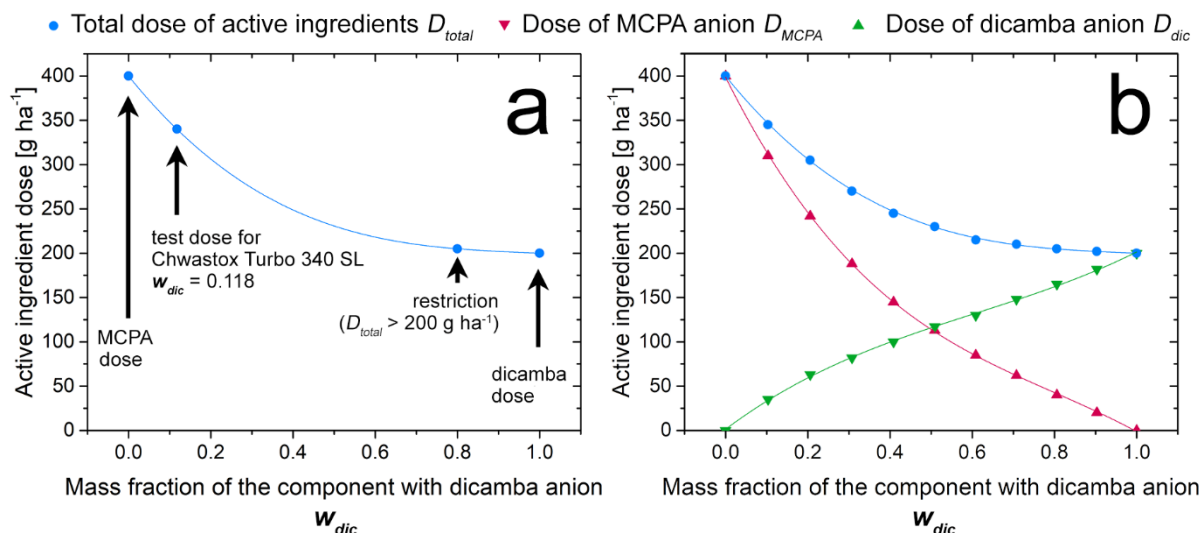
Figure 1. Determination of the total dose (D_{total}) of active ingredients for tested DSILs with varying molar fraction of dicamba anion (a) and values of the determined doses (total, MCPA anion only, and dicamba anion only) found for each mass fraction of the considered systems (b)

For each of the DSIL tested, a reference system consisting of both Chwastox Extra 300 SL and Dicash 480 SL in doses of an herbicidal anion equivalent to the determined non-standard doses of MCPA and dicamba anions in DSIL systems was prepared and tested.

Both single-anion ILs and DSILs, as well as the respective reference systems, were dissolved in water and applied with a moving sprayer (APORO, Poznan, Poland) by using a TeeJet VP 110/02 (TeeJet Technologies, Wheaton, IL, USA) with a flat-fan nozzle capable of delivering 200 dm^3 of spray solution per 1 ha at an operating pressure of 0.2 MPa. The sprayer was moved at a constant speed of 3.1 m s^{-1} at the height of 40 cm above the plants. The treated plants were subsequently placed in a greenhouse under the environmental conditions defined previously. Two weeks after treatment, the plants were cut at the soil level and weighed at 0.01 g accuracy. The results of the experiment were expressed in form of percent of the fresh weight reduction in comparison to the weight of control objects (plants untreated with any herbicidal formulations). Each error margin range represents standard errors of the mean (SEM). The SEM values were calculated according to following equation:

SEM = $s/n^{0.5}$

where SEM is the standard error of the mean, s is the sample standard deviation, and n is the number of replications. Data were statistically analyzed using one-way ANOVA with a random series effect. Fisher's multiple post hoc test ($\alpha = 0.05$) was used to compare treatments.

10

2.2.8. Toxicity towards freshwater algae

To determine the acute toxicity of the selected DSIL and its parent ILs, experiments were carried out on model *Chlorella vulgaris* (SAG 211-11b) cells obtained from Culture Collection of Algae at Göttingen University (Germany). The experiments was performed according to the methodology described in OECD 201 Guidelines.[29] Algae were cultivated in OECD TG medium prepared as described in the Annex 3 of the OECD 201 Guidelines in sterile conditions. To accommodate *C. vulgaris* to test conditions, algae cells have been cultured in OECD medium for 4 days before tests. The inoculum was continuously aerated with sterile air and illuminated with magenta (red + blue) LED grow light with the illuminance of 5500 ±800 lx. Before tests, inoculum was diluted with pure medium until its absorbance of monochromatic light (688 nm) was in the range of 0.05–0.08 at 10 cm path. To obtain the desired range of concentrations, 19 cm^3 portions of diluted inoculum were mixed with 1 cm^3 of the prepared toxicant solution in OECD medium. For control, 1 cm^3 of pure OECD medium was added. In the range finding tests, the selected IL and DSIL systems were tested in triplicates at a series of geometrically decreasing concentrations: 100, 10, 1, and 0.1 mg dm^{-3}. The absorbance at 688 nm was tested for each sample using 10 cm-long glass cuvettes, and the measurements were conducted at the start of the experiment and after 72 hours. The contents of all test vessels were mixed and illuminated continuously during the test, and their position was randomized to achieve similar levels of illumination for each sample throughout the experiment. The tests were conducted at 22–23 °C. The rate of inhibition of algae growth was calculated according to the eq. 7:

$$\mu = \frac{\ln(OD_{t_2}) - \ln(OD_{t_1})}{t_2 - t_1} \tag{7}$$

where OD_{t_2} and OD_{t_1} are the absorbances of the tested solution at the start (t_1) and at the end (t_2) of the experiment, respectively. Growth rate inhibition was then calculated in relation to the control mean:

$$I_r = 100 \cdot \left(1 - \frac{\mu_{sample}}{\mu_{control}}\right) \tag{8}$$

The EC$_{50}$ range for each of the toxicants tested was determined based on the relationship between its concentration and the calculated I_r value., To determine the exact EC$_{50}$ values, the experiments were replicated for each of the toxicants using the same methodology as described above, but different series of decreasing concentrations based on the EC$_{50}$ ranges found for each compound: 2.84, 2.13, 1.60, 1.20, 0.90, and 0.625 mg dm^{-3} for ILs comprising a single anion, and 1.60, 1.20, 0.80, 0.40, 0.20, and 0.10 mg dm^{-3} for the DSIL system. Based on the

11

concentration-I_r relationships and the analyses of dose-response curves plotted and approximated to the Hill equation, EC_{50} values were determined for each of the tested systems.

## 3. Results and discussion

3.1. Synthesis

Before the syntheses were conducted, 2-[2-(dimethylamino)ethoxy]ethanol was subsequently transformed into the source of IL cation, hexadecyl[2-(2-hydroxyethoxy)ethyl]dimethylammonium bromide (Scheme 1, Stage I). The quaternary ammonium salt was obtained according to a previously developed method.[25] However, based on FT-IR spectra acquired *in situ* during the synthesis, it was established that the quaternization product is formed in satisfactory amounts as early as 5 h after the start of the process – 1 hour less compared to previous reports.[25] The resulting bromide was isolated by filtration followed by washing with an apolar solvent, but originally used hexane was substituted by significantly safer heptane.[30] These changes made it possible to reduce the negative environmental impact of the process.
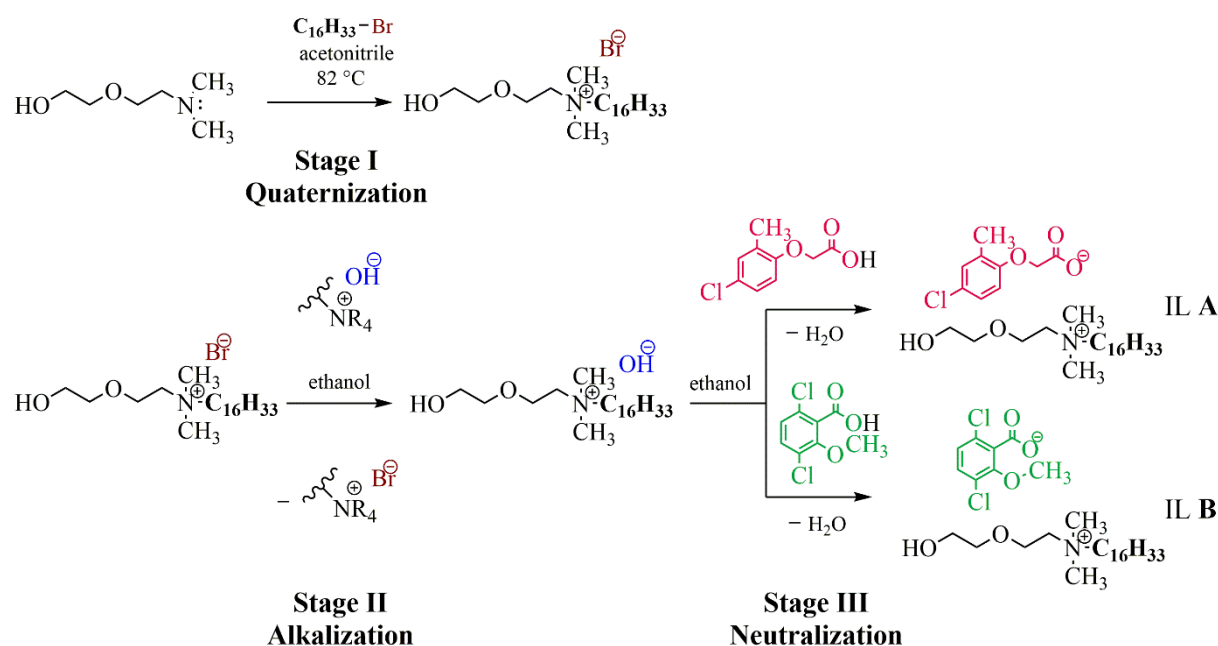
Scheme 1. Synthesis of quaternary ammonium bromide (Stage I) and ILs (Stage II and III)

Subsequently, the bromide anion in the obtained bromide was exchanged for either MCPA or dicamba anion to obtain two single-ion ILs: hexadecyl[2-(2-hydroxyethoxy)ethyl]dimethylammonium 4-chloro-2-methylphenoxyacetate (**A**) and hexadecyl[2-(2-hydroxyethoxy)ethyl]dimethylammonium 3,6-dichloro-2-methoxybenzoate (**B**), respectively. Both of these single-anion ILs were previously described[25,26] and the

12

process was conducted according to the known two-step methodology which consisted in alkalization of a quaternary bromide with anionic resin (Stage II) and subsequent neutralization of the formed hydroxide with the appropriate synthetic auxin (MCPA or dicamba) in acid form (Stage III), using naturally derived ethanol as a solvent.[26]

Stage IV
Formation of DSILs
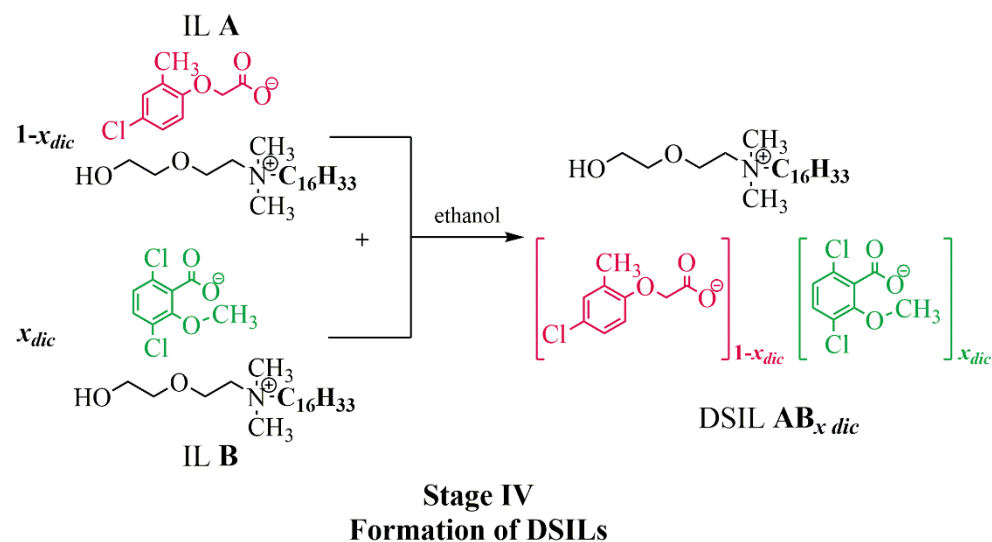
Scheme 2. Preparation of DSILs (Stage IV)

The basic properties of 9 new DSILs obtained in a simple homogenization (Stage IV, Scheme 2), as well as their parent ILs, are summarized in Table 1. To perform accurate spectroscopic studies, 2 additional DSILs with the highest molar fractions of dicamba ($AB_{0.95}$ and $AB_{0.99}$) were obtained by mixing $AB_{0.9}$ and **B** according to an analogous method. All of the obtained systems were colorless liquids at 25 °C.

Table 1. Synthesized ILs (**A**, **B**) and DSILs ($AB_{0.1}$–$AB_{0.99}$)

IL/DSIL	Anions	Molar fraction of the dicamba anion x_{dic}	Water content (initial) [%]	Water content (after drying) [%]	State at 25 °C
A	[MCPA]	0.00	6.115	1.402	liquid
$AB_{0.1}$	$[MCPA]_{0.9}[dicamba]_{0.1}$	0.10	6.400	1.234	liquid
$AB_{0.2}$	$[MCPA]_{0.8}[dicamba]_{0.2}$	0.20	3.885	1.681	liquid
$AB_{0.3}$	$[MCPA]_{0.7}[dicamba]_{0.3}$	0.30	5.095	1.219	liquid
$AB_{0.4}$	$[MCPA]_{0.6}[dicamba]_{0.4}$	0.40	5.232	1.795	liquid
$AB_{0.5}$	$[MCPA]_{0.5}[dicamba]_{0.5}$	0.50	5.394	1.129	liquid
$AB_{0.6}$	$[MCPA]_{0.4}[dicamba]_{0.6}$	0.60	4.657	0.914	liquid
$AB_{0.7}$	$[MCPA]_{0.3}[dicamba]_{0.7}$	0.70	4.281	0.798	liquid

13

AB$_{0.8}$	[MCPA]$_{0.2}$[dicamba]$_{0.8}$	0.80	3.899	0.756	liquid
AB$_{0.9}$	[MCPA]$_{0.1}$[dicamba]$_{0.9}$	0.90	4.294	0.637	liquid
AB$_{0.95}$	[MCPA]$_{0.05}$[dicamba]$_{0.95}$	0.95	-[a]	0.721	liquid
AB$_{0.99}$	[MCPA]$_{0.01}$[dicamba]$_{0.99}$	0.99	-[a]	0.833	liquid
B	[dicamba]	1.00	4.207	0.849	liquid

[a] Systems **AB$_{0.95}$** and **AB$_{0.99}$** were obtained from the previously dried ILs.

The formation of water during synthesis, combined with highly hygroscopic properties of ion exchange products, results in a high water content in the raw products (approximately 4–6%, Table 1) and difficulties in its removal. Such a high water content would significantly affect and alter analysis of the physicochemical properties of the obtained DSILs (*e.g.*, density, refractive index).[31–33] Therefore, an effort was made to remove most of the water from the DSILs *via* a two-step azeotropic distillation. Thorough removal of solvents was facilitated by subsequent drying of the residue using a Schlenk line with a vacuum of approximately $2 \cdot 10^{-5}$ bar.
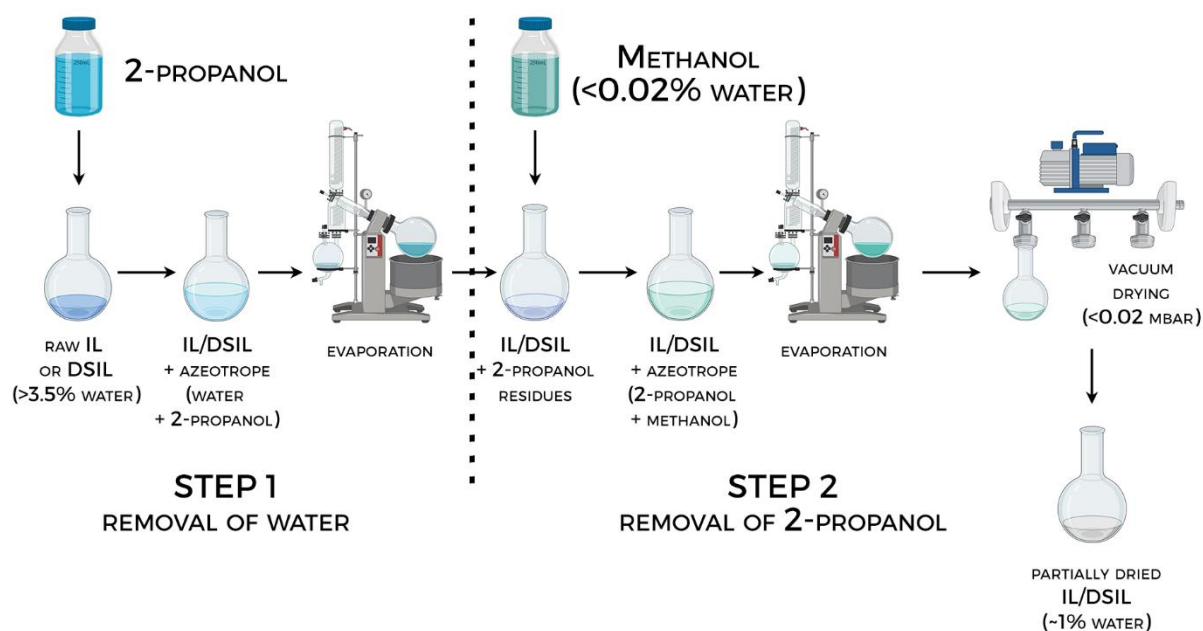
**Figure 2.** Removal of water from ILs and DSILs using two-step azeotropic distillation method

As a result of the above method, it was possible to significantly reduce the amount of water in the obtained DSILs: from 2.5 times (**AB$_{0.2}$**) up to 6.5 times (**AB$_{0.9}$**). The exact water contents after drying the systems are summarized in Table 1, they ranged from 0.6% (**AB$_{0.9}$**) to 1.7% (**AB$_{0.2}$**). It is likely that this is due to an increase in the strength of DSIL–water hydrogen bonding as the molar proportion of the MCPA anion increases. Drying process revealed that the remaining water must be therefore relatively highly bound with the ionic system. Further

14

dehydration of such highly hygroscopic DSILs would require sophisticated methods, and conducting further analyses would have to take place in a dry inert gas atmosphere to achieve substantially reduced water contents (<2000 ppm) demonstrated in other reports. However, it should be borne in mind that the obtained ILs are intended for use in aqueous solutions, thus the increased water content in raw products does not constitute significant issue from a point of view of their industrial application.

3.2. Spectral analysis

Detailed ^{1}H NMR spectra of each system and ^{13}C NMR and FT-IR spectra of ILs **A** and **B** as well as selected DSILs (**AB$_{0.2}$**, **AB$_{0.4}$**, **AB$_{0.6}$**, and **AB$_{0.8}$**) are summarized in Supplementary Data (Figs. A.1–A.26). The analysis of the NMR spectra allowed for determination of accuracy of the molar ratio between the utilized biologically active anions.[26] Moreover, clear changes in the intensity of signals originating from carbon atoms in both anions were observed in the ^{13}C NMR spectra, coinciding with variations in their molar fractions, while signals from the common cation were characterized by equal intensity on all ^{13}C NMR spectra. As shown in previous ^{1}H NMR spectra analyses,[34–37] that are consistent with our studies,[25,26,38] some hydrogen atoms in IL mixtures (particularly those in the vicinity of the charged atoms) alter their chemical shifts compared to the respective atoms of pure single-anion ILs. Therefore, we thoroughly analyzed the changes in chemical shifts for the signals in the ^{1}H NMR spectra for all the ILs and DSILs obtained, taking into account the increasing x_{dic} value. We observed that an increase in the amount of dicamba in the DSILs has a particularly pronounced effect on the chemical shift of the signal coming from the methylene group in the MCPA anion (highlighted in Fig. 3a, comparison of the whole ^{1}H NMR spectra for **A**, **AB$_{0.1}$**–**AB$_{0.99}$** and **B** is provided in Fig. A.27, Supplementary Data), which is in close proximity to the carboxylate moiety (3 bonds away from the negatively charged oxygen atoms in the MCPA anion). The dependence of the chemical shift change on the molar fraction of the dicamba anion x_{dic} is exponential, and at x_{dic} = 0.99 (**AB$_{0.9}$**) the signal appeared at a chemical shift of 4.393 ppm – 0.256 ppm more compared to the single-anion IL containing MCPA only (**A**, x_{dic} = 0.0). We observed a similar, but approximately three times weaker increase for the signal coming from the hydrogen atom in the α position to the 2-hydroxy-2-oxomethoxyl substituent in the aromatic ring, 6 bonds away from the negatively charged oxygen atoms – from 6.655 (**A**) to 6.718 ppm (**AB$_{0.99}$**). More detailed analysis of the lesser chemical shift changes observed for other hydrogen atoms in the MCPA anion is provided in Supplementary Data (pages A.30–A.32, Tables A.3–A.4). The recorded data clearly indicate that the competing anion-anion interactions are responsible for the phenomenon of deshielding of hydrogen atoms that increases as the molar ratio of the

15

competing anion (dicamba in the analyzed DSIL system) rises. It should be noted here that the greater the number of chemical bonds between a given hydrogen atom and the moiety on which the negative charge is localized, the lower the intensity of the phenomenon described (Fig. A.28, Supplementary Data).
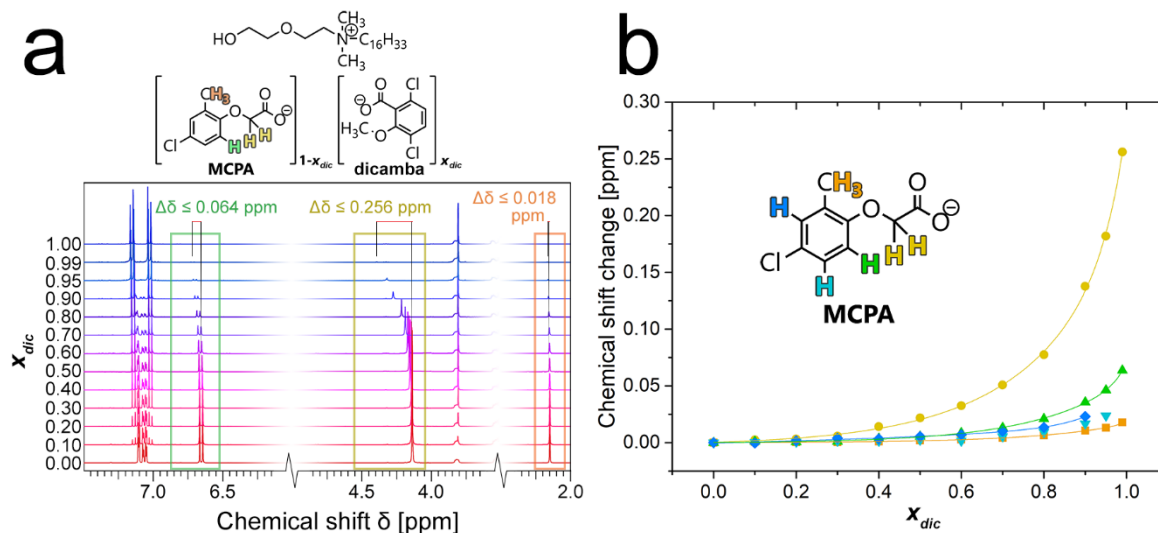
Figure 3. Changes in the ^{1}H NMR spectra acquired for **A**, **AB$_{0.1}$**–**AB$_{0.99}$** and **B** (a) and the dependency of chemical shift changes for hydrogen atoms in the MCPA anion on x_{dic} value (b)

Of the considerable number of determined relationships of chemical shift changes with x_{dic} value, the MCPA methylene group shift dependency visible in Fig. 3b has the largest difference in the value of the dependent variable (chemical shift) and can be approximated to an exponential function with the following formula:

$$\delta = \delta_0 + A_1 exp^{\frac{x_{dic}-x_{dic\cdot0}}{t_1}} + A_2 exp^{\frac{x_{dic}-x_{dic\cdot0}}{t_2}} \qquad (9)$$

where δ_0 is a chemical shift value recorded for **A** (see Table A.3, Supplementary Data). Therefore, with the known characteristics of this dependence, ^{1}H NMR analysis proves to be an excellent auxiliary tool for determining unknown molar fraction values of DSIL components not only based on band integration, but also on the basis of chemical shifts of known signals in the spectrum.

Found values of the equation parameters given above are provided in Table A.4 (Supplementary Data). The approximation above is characterized by a very high R^2 value (0.999) in the investigated range of dicamba molar fraction from 0.0 to 0.99.

The corresponding chemical shifts changes in the other ions present in the obtained systems (the dicamba anion and the hexadecyl[2-(2-hydroxyethoxy)ethyl]dimethylammonium cation) were also analyzed. They were far less pronounced compared to the signal from the methylene

16

group in the MCPA anion described above, and are described in detail in the Supplementary Data (for the dicamba anion: pages A.33–A.34, Fig. A.29, Table A.5, for the cation: pages A.35–A.36, Fig. A.30, Tables A.6–A.7).

The influence of the dicamba molar ratio of the DSILs analyzed on the changes in the chemical shifts, evident in the ^{1}H NMR spectra for all 3 ions present in the systems to some extent, is imperceptible in the ^{13}C NMR spectra. The performed analysis showed that the signals from the same carbon atoms occur at nearly identical chemical shifts (max. ±0.2 ppm). Moreover, these changes exhibit no correlation with x_{dic} value. For example, in the case of the signal originating from the carbon atom in the CH_2 group in the MCPA anion it occurs at almost the identical chemical shift around 67.9–68.2 ppm, with the σ value increasing as follows: **AB$_{0.8}$** < **A** < **AB$_{0.4}$** ≈ **AB$_{0.6}$** < **AB$_{0.2}$**. This phenomenon shows that the effect of the molar fraction change of the competing anion in the DSIL system on the chemical environment of the carbon atoms cannot be unequivocally determined. The FT-IR analysis of obtained ILs and DSILs indicates the presence of all the characteristic bands derived from the cation and from both anions in the collected spectra. We also noted the rise of intensity of the bands derived from the dicamba anion along with increase in x_{dic} value. This effect is evident in the highlighted regions on a comparison of FT-IR spectra from **A**, **AB$_{0.5}$** and **B**, which are shown together in Fig. A.31 (Supplementary Data). The occurrence on each of the analyzed spectra of a broad signal of high intensity in the range from 3650 to 3050 cm^{-1} originating from stretching vibrations in the O–H bonds is indicated by the formation of numerous hydrogen bonds, most likely both between the ions of the analyzed systems, and also between the hydroxyl group and water that remains in the ILs and DSILs after drying.
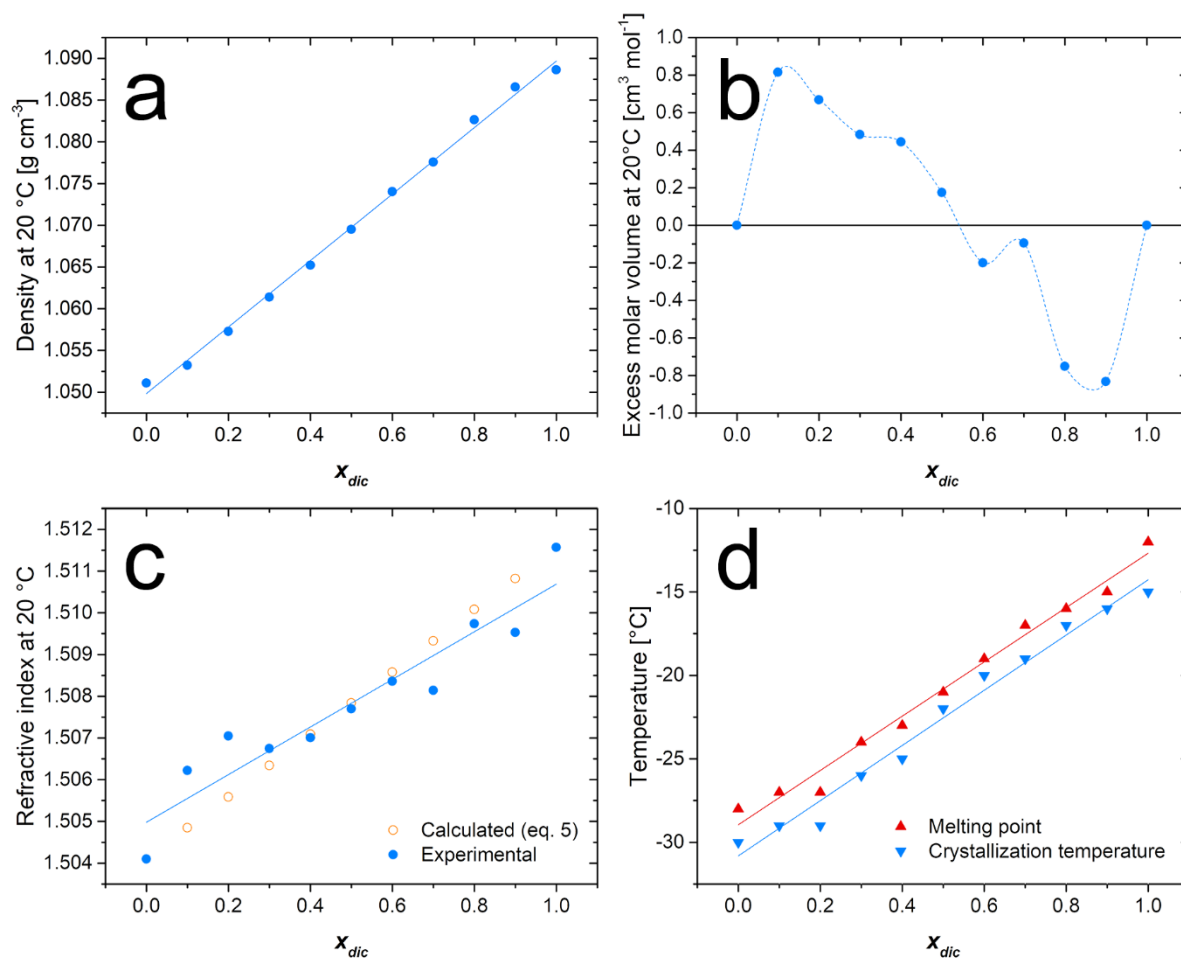

3.3. Physicochemical properties

The following basic physicochemical properties were studied for both single-ion ILs (**A**, **B**) and DSILs (**AB$_{0.1}$**–**AB$_{0.9}$**): density and refractive index at 20 °C, as well as the characteristics of phase transformations in the temperature range from -80 °C to 120 °C. The two single-anion ILs exhibited values of density equal to 1.0511 (**A**) and 1.0886 g cm^{-3} (**B**), while all the studied DSILs possessed densities between these two values. The density dependence of x_{dic} is shown in Fig. 4a (detailed data are summarized in Table A.8, Supplementary Data). These results showed that there is a close correlation between the density at 20 °C and the molar proportion of the dicamba anion (x_{dic}) in a given system; across the x_{dic} range, a 0.1 increase in this parameter resulted in an increase in DSIL density of approximately 0.0038 g cm^{-3}. This relationship can be approximated to a linear function with very high accuracy ($R^2 = 0.997$), with

exact regression parameters provided in Table A.9 in Supplementary Data. The obtained results are consistent with previous studies on multi-ion ILs,[11,28,39] where such systems have often been reported as having good correlation with a linear mixing law.[12]

Since the average molar mass of ILs and DSILs (M_w) increases proportionally with increasing x_{dic}, it should be emphasized that a close linear relationship also exists between the average molar mass of systems **A**, **AB$_{0.1}$**–**AB$_{0.9}$** and **B** and their measured density. This is confirmed by the fact that all analyzed systems are characterized by a very similar molar volume (V_m^{20}), defined as the quotient of the molar mass of a substance and its density at a given temperature. The average value of this parameter for all ILs and DSILs is approx. 531.4 cm^3 mol^{-1}, and the calculated extreme values (530.7 cm^3 mol^{-1} for **AB$_{0.9}$** and 532.0 cm^3 mol^{-1} for **AB$_{0.1}$**) differ from the average value by about 0.1%. It should be noted here that DSILs containing a higher molar proportion of MCPA anion (**AB$_{0.1}$**–**AB$_{0.5}$**) have positive excess molar volume (V_m^{E20}) values than the average, while at higher x_{dic} values V_m^{E20} values fall below zero. This relationship is shown in Fig. 4b. Positive values of V_m^{E20} indicate the presence of non-additive physical contributions in the analyzed system, including non-specific interactions between mixture components that alter the molar volume, while negative values are associated with chemical or structural interactions (*e.g.*, changes in coulombic interactions or hydrogen bonds between mixture components, changes in free volume or ion packing).[28] Thus, it can be predicted that an increase in the molar proportion of the dicamba anion above 0.5 plausibly causes a significant change in the nature of the interactions in DSIL. These changes may affect the chemical environment of MCPA anions, which explains the observed deshielding of hydrogen atoms in NMR spectra.

The negligible differences between V_m^{20} values also indicate that other parameters proportional to this physical quantity also have similar values. The average volume occupied by a single ion pair of a given system (V_{ip}^{20}) is nearly identical (from 0.881 nm^3 for **AB$_{0.9}$** to 0.883 nm^3 for **AB$_{0.1}$**) in all analyzed cases. Moreover, there are no significant differences between the studied ILs and DSILs systems in terms of lattice energy at 20 °C (U_{POT}^{20}) and standard molar entropy ($S^{\circ 20}$) values.

18

Figure 4. Relationships of physicochemical properties of ILs and DSILs with x_{dic} parameter: density at 20 °C (a), excess molar volume at 20 °C (b), refractive index at 20 °C (c), and melting points and crystallization temperatures (d)

As in the case of density, values of the refractive index at 20 °C (n_D^{20}) took extreme values for single parent ILs: 1.5041 for **A** and 1.5116 for **B**, whereas the refractive indices of DSILs occurred within this range. Detailed results are given in Table A.8 (Supplementary Data). However, the linear correlation of the refractive index with x_{dic} is not as accurate as in the case of density; the R^2 value is equal to 0.888 (Fig. 4c). It should be noted here that the experimental values for DSILs containing similar or the same proportion of MCPA anions as dicamba (**AB_{0.4}**–**AB_{0.6}**) were close to the theoretical ones. Thus, the relationship between Δn_D^{20} and x_{dic} followed a similar pattern as the dependence of excess molar volume (V_m^{E20}) on the molar fraction of dicamba. This corroborates with a known relationship between density and refractive index: with a higher density of a substance, the spatial packing of its chemical constituents increases, and refraction results from the interaction of light with molecules (or ions).[40]

19

The phase transitions of the studied systems were also determined using the differential scanning calorimetry technique. For both parent ILs **A** and **B**, as well as all systems containing MCPA and dicamba (**AB$_{0.1}$**–**AB$_{0.9}$**), melting (T$_m$) and crystallization (T$_c$) temperatures were observed during heating and cooling cycles, respectively. The thermograms are available on Figs. A.32–A.42 (Supplementary Data), while values of the phase transition temperatures are summarized in Table A.10 (Supplementary Data). The presence of a long hexadecyl substituent in the cation of ILs and DSILs significantly reduced lattice energy. This is evidenced by the fact that analogous MCPA and dicamba salts with shorter substituents in the cation underwent only glass transition at temperatures lower than -30 °C.[25] As shown in Fig. 4d, the observed T$_m$ values ranged from -28 °C (IL **A**) and rose with increasing x_{dic} value up to -12 °C for **B**. Thus, the melting point reduction typical of eutectic mixtures was not observed for DSILs. The crystallization temperatures (T$_c$), on the other hand, for each of the studied systems were 1–3 °C lower than the corresponding T$_m$ values. The dependence of both phase transformation temperatures on x_{dic} can be approximated to a linear function with high accuracy (R^2 > 0.98).

3.4. Surface activity

In binary systems or mixtures, the ratio of components has a notable impact on surface activity. In this study, the critical micelle concentration (CMC) and surface tension at CMC for ILs **A** and **B** and DSILs at various molar ratios (**AB$_{0.1}$**–**AB$_{0.9}$**) were determined. The obtained data is depicted in Fig. 5, and the exact values are provided in Table A.11 (Supplementary Data).
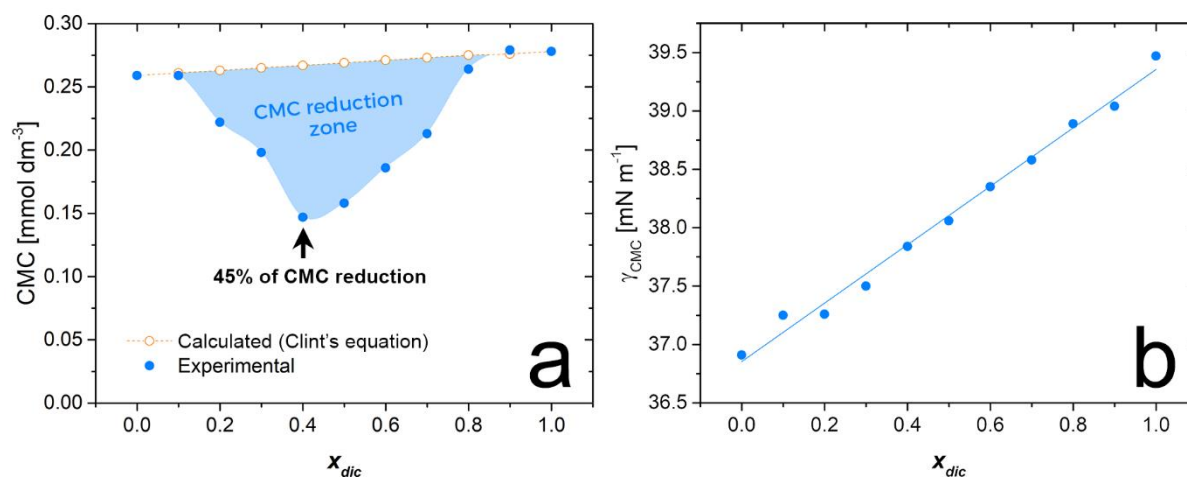
Figure 5. Relationships between CMC (a) and surface tension at CMC (b) with molar fractions of dicamba anion x_{dic} in ILs and DSILs.

A non-linear dependency of CMC on the x_{dic} was established in the analyzed compositions. The CMC for DSILs with a molar fraction of dicamba anion ranging from 0.2 to 0.8 exhibited significant deviation from the theoretical CMC values of binary mixtures calculated according

20

to the Clint's equation (Fig. 5a; the deviation is visualized as a blue area).[41–43] The most notable discrepancy was observed for the DSIL $AB_{0.4}$, where the experimental CMC value was as much as 45% lower compared to the theoretical one. Similar deviations from the "ideal" binary mixture behaviour were also observed previously for mixtures of anionic/cationic[44] and ionic/non-ionic[45] surfactants. These non-additive effects in surfactant mixtures predominantly stem from the entropy of the diffuse counter-ion layer outside the micelle interfacial boundaries, as well as the length of the tails and the charges in the cation and anion.[45,46]

The occurrence of the above-described synergistic effect in DSILs makes it a legitimate strategy to combine two active surfactants in well-defined ratios to reduce the amount of surfactants introduced into the environment. Synthetic auxins show higher efficiency when applied in the form of aqueous solutions with the addition of a surface-active adjuvant, therefore, such DSILs with a surface-active cation and pesticidal anions can guarantee excellent efficacy without necessity of use any other additives.[25,47] Furthermore, the analysis of the surface tension of the aqueous solution for the DSILs $AB_{0.1}$–$AB_{0.9}$ and ILs A and B at their respective CMCs indicated a linear dependence on the x_{dic} value, as illustrated in Fig. 5b. No significant deviation from the linear relationship ($R > 0.98$) indicates lack on any unexpected interactions in the analyzed systems with water and air.[48]

3.5. Greenhouse experiments

To determine the ability of the DSILs obtained from two popular herbicides, greenhouse experiments were performed on common lambsquarters – a plant susceptible to both, MCPA and dicamba, accordingly. It should be noted that dicamba is characterized by higher activity towards dicotyledonous weeds compared to MCPA, so the dose of both active agents differed. The method of determining D_{total} value for systems with different proportions of the dicamba anion is visualized in Fig. 1. Both parent ILs A and B, and 4 of the obtained DSILs: $AB_{0.2}$, $AB_{0.4}$, $AB_{0.6}$, and $AB_{0.8}$ were selected for greenhouse experiments. Reference products – commercially available herbicide formulations (mix of Chwastox Extra 300 SL and Dicash 480 SL) were used at the same molar ratio of active ingredients and concentrations as the ILs and DSILs. The obtained results are illustrated in Fig. 6, and the exact values of fresh weight reduction are given in Table A.12 (Supplementary Data).
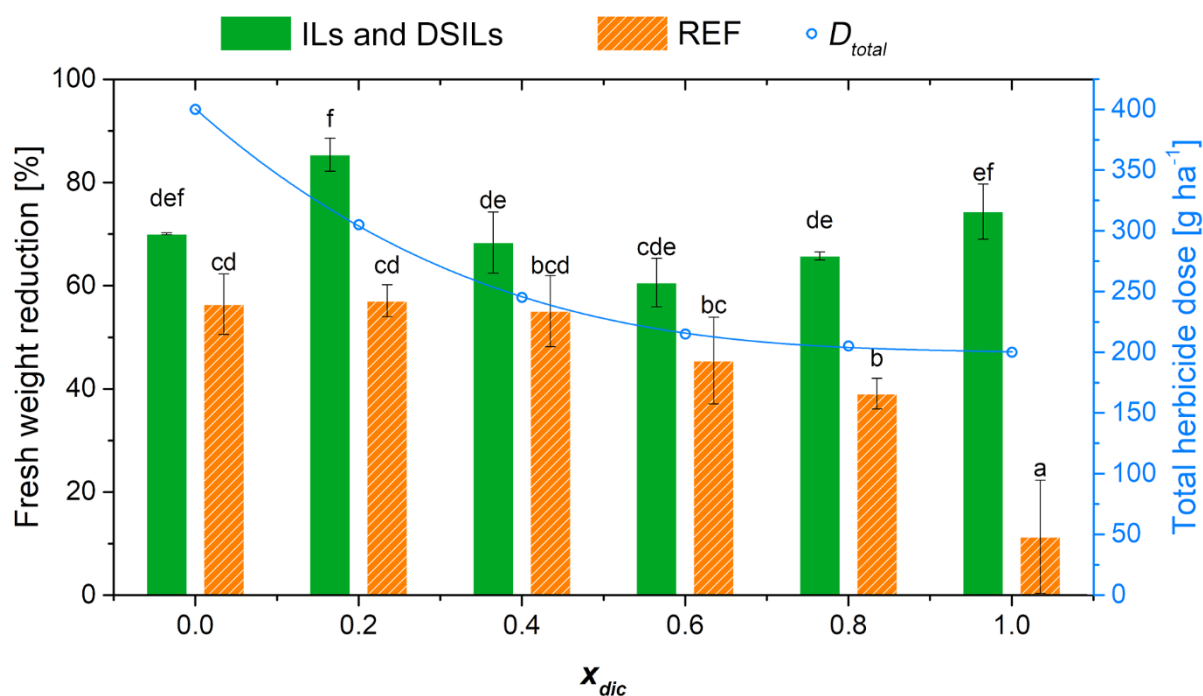
Figure 6. Herbicidal efficiency of the obtained ILs and DSILs compared with reference formulations (REF) with the same molar ratios of the active ingredients (MCPA and dicamba)

The applied ILs or DSILs were capable of reducing the fresh weight of lambsquarters plants in the range from 61% (**AB$_{0.6}$**) to 86% (**AB$_{0.2}$**) compared to the fresh weight of control objects, while the commercially available herbicides or their tank mixes were characterized by lower activity in the range from 11% to 57%. These findings indicate that not only ILs but also DSILs were characterized by higher biological activity compared to the reference formulations. In the case of **AB$_{0.2}$**, **AB$_{0.8}$**, and **B**, these differences were statistically significant. It should also be noted that **AB$_{0.8}$**, and **B** were able to inhibit the growth of test plants 2 times and 7 times more effectively, respectively, compared to the reference herbicides. This increased herbicidal activity is mainly due to surface activity of the cation and the improved wettability of the leaves.[49] The data of the contact angle of the aqueous solutions of ILs and DSILs, which were applied in the greenhouse experiments, on the model hydrophobic surface (paraffin) are presented in Table A.11 in Supplementary Data. These data indicate that all the systems tested were capable of reducing the contact angle of their aqueous solution to values in the range of 71–77°, which is approximately 35–40° less compared to the contact angle of water on hydrophobic paraffin surface.[50]

The DSIL systems containing a significant molar proportion of dicamba anion (*x$_{dic}$* = 0.4 or more, *i.e.* **AB$_{0.4}$**, **AB$_{0.6}$**, and **AB$_{0.8}$**) were capable of reducing the fresh weight of test plants at an analogous level to single-anion IL **A** containing only MCPA at a higher dose. This result

22

means that the addition of dicamba allows the reduction of the MCPA dose in DSILs with higher x_{dic} values to be fully compensated, and also confirms that the proposed method of selecting the total dose of both herbicides (D_{total}) proved to be correct.

Noteworthy, DSIL $AB_{0.2}$ exhibited the highest biological activity of all studied systems, and its application resulted in an 85% reduction in fresh weight of the test plants compared to the control. This result, indicating the possibility of effective control of common lambsquarters growth in the crop, was clearly superior to other tested active forms. For larger x_{dic} values, the addition of dicamba is able to compensate for the significant loss of MCPA, but it does not result in a clear improvement in DSIL activity. Moreover, the compensation effect facilitates the use of DSILs at lower doses of the active ingredient. $AB_{0.2}$ applied at a reduced total dose of 305 g of a.i. per ha enables slightly better results compared to the application of the IL A (with MCPA anion only) at a higher dose (400 g ha^{-1}). These results confirm our previous findings, in which it was revealed that the DSIL containing the same cation and anions of MCPA and its less biologically active analog, mecoprop-P, along with a small addition of dicamba.[26] Effectiveness at the level of 85% for $AB_{0.2}$, with a 30% reduction in the dose of active ingredients compared to the recommended doses of commercial formulations indicates the possibility of common lambsquarters control in a crop production, while also reducing the amount of pesticides released into the environment.

3.6. Ecotoxicity studies

Since the application of $AB_{0.2}$ resulted in the greatest efficacy towards the tested dicotyledonous plant, it was also necessary to analyse its potential threat to non-target organisms. It is assumed that only 5% of active substances of herbicide formulations interact with target organisms, while the remaining 95% affects non-target organisms or penetrates the environment, either accumulating in the soil or leaching into groundwater.[51] In addition, it is well known that cationic surfactants exhibit very high toxicity to aquatic organisms. For example, benzalkonium chloride, popularly used as an active ingredient in disinfectant formulations, exhibits very high acute toxicity to freshwater crustaceans (*Daphnia magna*, EC_{50} = 0.016 mg dm^{-3}),[52] algae (*Chlorella vulgaris*, EC_{50} up to 0.0576 mg dm^{-3})[53] or fish (*Oncorhynchus mykiss*, gill cell line-W1, EC_{50} = 0.31 mg dm^{-3}).[52]

To provide a preliminary evaluation of the risks associated with obtaining ILs and DSILs with a surface-active amphiphilic cation, an acute toxicity analysis was performed using a model organism from the freshwater algae group, *C. vulgaris*. The study was performed for both parent ILs, A and B, as well as DSIL $AB_{0.2}$. Based on the analysis of the obtained dose-response

curves, EC_{50} values were determined for each of the tested systems (Fig. 7 and Table A.13 in Supplementary Data).
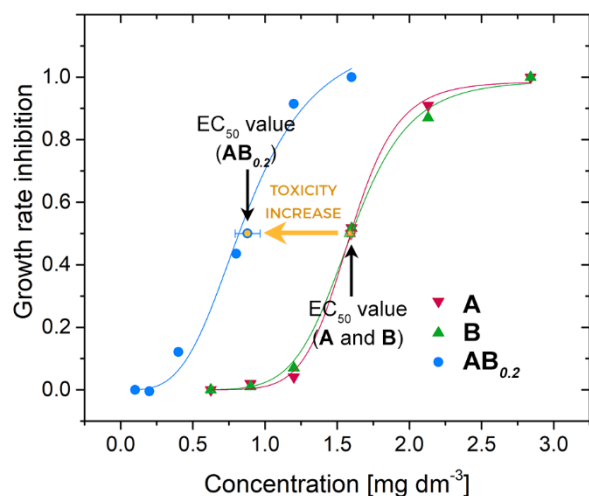
Figure 7. Dose-response curves and EC_{50} values determined for **A**, **AB$_{0.2}$** and **B** based on *C. vulgaris* acute toxicity tests

The results show that **A** and **B** exhibited virtually the same toxicity profile against *C. vulgaris* (EC_{50} = 1.60 mg dm^{-3} for **A** and 1.59 mg dm^{-3} for **B**). This allows to classify both ILs to Category II substances in terms of aquatic hazards according to the GHS. The similar toxicity of compounds **A** and **B** indicates that the chemical structure of synthetic auxin in the anion (dicamba or MCPA) has no significant effect on ecotoxicity. It has been discovered that compounds from the auxin group are also produced by other groups of organisms, including bacteria, fungi or algae.[54] It is postulated that auxins in algae play a similar role to those in higher plants, stimulating cell division and growth of algal colonies.[55] Consequently, herbicidal substances from the group of synthetic auxins (including MCPA and dicamba) were characterized by low toxicity to algae,[56] while cationic surfactants are known for their high toxicity to algae,[57] primarily due to their ability to adsorb to their cell membranes.[58]

For the **AB$_{0.2}$**, a noticeable increase in acute toxicity toward *C. vulgaris* compared to ILs **A** and **B** was observed. The determined EC_{50} value was equal to 0.88 mg dm^{-3}. Considering the mechanism of surfactant toxicity against algal cells, the increased ecotoxicity of **AB$_{0.2}$** is most likely due to the previously described surface activity enhancement on the interfacial surface, which causes the DSILs to have lower CMC compared to their parent ILs. However, the analyzed DSIL exhibits lower toxicity towards *C. vulgaris* compared to conventional quaternary ammonium salts with a substituent of the same length: cetyltrimethylammonium chloride (CTAC, EC_{50}: 0.14 mg dm^{-3}) or benzyldimethylhexadecylammonium chloride

24

(BAC$_{16}$, EC$_{50}$: 0.16 mg dm^{-3}).[53] This type of activity also indicates additional potential for the use of **AB$_{0.2}$** as an algicide (*e.g.*, to counteract algal growth in pools or ponds) at well-defined concentrations. Algicides are also used to counteract the eutrophication in natural water bodies. One of the most commonly used substances to counteract algal growth is copper(II) sulfate, however, this compound exhibits considerable toxicity to other aquatic organisms. Moreover, copper accumulates in the environment and can be dangerous to human health, so the search for less toxic alternatives is warranted.[59]

4. Conclusions

In the course of the present study, a series of new double salt ionic liquids (DSILs) were successfully obtained by simple homogenization of two known ILs comprising hexadecyl[2-(2-hydroxyethoxy)ethyl]dimethylammonium cation and two anions with herbicidal activity (MCPA or dicamba). Prepared DSILs contained different molar ratios between MCPA and dicamba ions, ranging from 9:1 (90% of MCPA) to 1:99 (1% of MCPA) in respective system. Spectral analysis confirmed that the formation of DSILs causes a change in the chemical environment of specific groups of atoms in the tested ions. In ^{1}H NMR spectra such alterations occurred as a significant difference in the chemical shifts of specific signals. The melting points of the analyzed DSIL systems were lower than -15 °C, which allows them to be classified as room-temperature ionic liquids. Fascinatingly, the determined critical micelle concentration (CMC) values for DSILs comprising MCPA:dicamba in a molar ratio from 2:8 to 8:2 were characterized by significantly lower values compared to the expected results from mixing law. The greatest reduction in CMC value (lower by 45% compared to assumptions) was observed for DSIL containing MCPA:dicamba in a molar ratio amounting to 6:4. Thus, the strategy involving formation of these surface-active DSILs may allow for effective reduction of the amount of surfactants or active agent used for treatment.

All DSILs evaluated for herbicidal efficacy against common lambsquarters showed similar efficacy compared to parent ILs with a single anion (MCPA or dicamba). These results indicate that there were no noticeable synergistic effects for the analyzed systems comprising large amounts of dicamba anion. Interestingly, the system containing a smaller amount of dicamba (MCPA:dicamba in a molar ratio amounting to 8:2) exhibited the highest biological activity within all the active substances tested and achieved 85% of fresh weight reduction compared to control. It can be concluded that a small addition of dicamba can more than compensate for the loss of MCPA dose. Therefore, the total dose of pesticide can be effectively reduced up to 25%

25

(from 400 to 305 g ha^{-1}) without any loss of efficacy. Most likely, the occurring synergistic effects cause a noticeable increase in the toxicity of this system towards *C. vulgaris* compared to parent ILs. This result confirms that a more thorough evaluation of the ecotoxicity of new compounds is crucial in the process of development of novel herbicidal formulations that are not only effective in use but also safe for non-target species.

Author contributions: CRediT

Tomasz Rzemieniecki: Conceptualization, Data curation, Formal analysis, Funding acquisition, Investigation, Methodology, Project administration, Resources, Visualization, Writing – original draft. **Damian K. Kaczmarek**: Data curation, Funding acquisition, Investigation, Methodology, Writing – original draft. **Witold Stachowiak**: Formal analysis, Methodology. **Katarzyna Marcinkowska**: Investigation, Methodology, Resources. **Michał Niemczak**: Funding acquisition, Resources, Writing – review & editing.

Funding sources

Appendices

Appendix A: Supplementary Data

References

[1] J. Afonso, A. Mezzetta, I.M. Marrucho, L. Guazzelli, History repeats itself again: Will the mistakes of the past for ILs be repeated for DESs? From being considered ionic liquids to becoming their alternative: the unbalanced turn of deep eutectic solvents, Green Chem. 25 (2023) 59–105. https://doi.org/10.1039/D2GC03198A.

[2] B. Kudłak, K. Owczarek, J. Namieśnik, Selected issues related to the toxicity of ionic liquids and deep eutectic solvents—a review, Environ. Sci. Pollut. Res. 22 (2015) 11975–11992. https://doi.org/10.1007/s11356-015-4794-y.

[3] S. Magina, A. Barros-Timmons, S.P.M. Ventura, D. V Evtuguin, Evaluating the

hazardous impact of ionic liquids – Challenges and opportunities, J. Hazard. Mater. 412 (2021) 125215. https://doi.org/10.1016/j.jhazmat.2021.125215.

[4]   V.G. Maciel, D.J. Wales, M. Seferin, C.M.L. Ugaya, V. Sans, State-of-the-art and limitations in the life cycle assessment of ionic liquids, J. Clean. Prod. 217 (2019) 844–858. https://doi.org/10.1016/j.jclepro.2019.01.133.

[5]   Y. Liu, Z. Dai, Z. Zhang, S. Zeng, F. Li, X. Zhang, Y. Nie, L. Zhang, S. Zhang, X. Ji, Ionic liquids/deep eutectic solvents for CO_2 capture: Reviewing and evaluating, Green Energy Environ. 6 (2021) 314–328. https://doi.org/10.1016/j.gee.2020.11.024.

[6]   J. Sun, Y. Sato, Y. Sakai, Y. Kansha, A review of ionic liquids and deep eutectic solvents design for CO_2 capture with machine learning, J. Clean. Prod. 414 (2023) 137695. https://doi.org/10.1016/j.jclepro.2023.137695.

[7]   K. Zhang, J. Wu, H. Yoo, Y. Lee, Machine Learning-based approach for Tailor-Made design of ionic Liquids: Application to CO_2 capture, Sep. Purif. Technol. 275 (2021) 119117. https://doi.org/10.1016/j.seppur.2021.119117.

[8]   P. Dhakal, J.K. Shah, A generalized machine learning model for predicting ionic conductivity of ionic liquids, Mol. Syst. Des. Eng. 7 (2022) 1344–1353. https://doi.org/10.1039/D2ME00046F.

[9]   S.P. Ijardar, R.L. Gardas, Chapter 16 - A physicochemical investigation of ionic liquid mixtures, in: J. Akhter Siddique, A. Ahmad, M.B.T.-I.L. and T.A. in G.C. Jawaid (Eds.), Adv. Green Sustain. Chem., Elsevier, 2023: pp. 289–312. https://doi.org/10.1016/B978-0-323-95931-5.00019-1.

[10]   M.A.R. Martins, G. Sharma, S.P. Pinho, R.L. Gardas, J.A.P. Coutinho, P.J. Carvalho, Selection and characterization of non-ideal ionic liquids mixtures to be used in CO_2 capture, Fluid Phase Equilib. 518 (2020) 112621. https://doi.org/10.1016/j.fluid.2020.112621.

[11]   H. Niedermeyer, J.P. Hallett, I.J. Villar-Garcia, P.A. Hunt, T. Welton, Mixtures of ionic liquids, Chem. Soc. Rev. 41 (2012) 7780–7802. https://doi.org/10.1039/C2CS35177C.

[12]   G. Chatel, J.F.B. Pereira, V. Debbeti, H. Wang, R.D. Rogers, Mixing ionic liquids – "simple mixtures" or "double salts"?, Green Chem. 16 (2014) 2051–2083. https://doi.org/10.1039/C3GC41389F.

[13]   F. Oyoun, A. Toncheva, L.C. Henríquez, R. Grougnet, F. Laoutid, N. Mignet, K. Alhareth, Y. Corvis, Deep Eutectic Solvents: An Eco-friendly Design for Drug Engineering, ChemSusChem 16 (2023) e202300669.

https://doi.org/10.1002/cssc.202300669.

[14] T. Swebocki, A.M. Kocot, A. Barras, H. Arellano, L. Bonnaud, K. Haddadi, A.-L. Fameau, S. Szunerits, M. Plotka, R. Boukherroub, Comparison of the Antibacterial Activity of Selected Deep Eutectic Solvents (DESs) and Deep Eutectic Solvents Comprising Organic Acids (OA-DESs) Toward Gram-Positive and Gram-Negative Species, Adv. Healthc. Mater. 13 (2024) 2303475. https://doi.org/10.1002/adhm.202303475.

[15] X. Wu, Q. Zhu, Z. Chen, W. Wu, Y. Lu, J. Qi, Ionic liquids as a useful tool for tailoring active pharmaceutical ingredients, J. Control. Release 338 (2021) 268–283. https://doi.org/10.1016/j.jconrel.2021.08.032.

[16] M. Handa, W.H. Almalki, R. Shukla, O. Afzal, A.S.A. Altamimi, S. Beg, M. Rahman, Active pharmaceutical ingredients (APIs) in ionic liquids: An effective approach for API physiochemical parameter optimization, Drug Discov. Today 27 (2022) 2415–2424. https://doi.org/10.1016/j.drudis.2022.06.003.

[17] J.L. Shamshina, R.D. Rogers, Ionic Liquids: New Forms of Active Pharmaceutical Ingredients with Unique, Tunable Properties, Chem. Rev. 123 (2023) 11894–11953. https://doi.org/10.1021/acs.chemrev.3c00384.

[18] K.S. Egorova, A. V Kibardin, A. V Posvyatenko, V.P. Ananikov, Mechanisms of Biological Effects of Ionic Liquids: From Single Cells to Multicellular Organisms, Chem. Rev. 124 (2024) 4679–4733. https://doi.org/10.1021/acs.chemrev.3c00420.

[19] A.J. Diggle, P.B. Neve, F.P. Smith, Herbicides used in combination can reduce the probability of herbicide resistance in finite weed populations, Weed Res. 43 (2003) 371–382. https://doi.org/10.1046/j.1365-3180.2003.00355.x.

[20] S.B. Powles, Q. Yu, Evolution in Action: Plants Resistant to Herbicides, Annu. Rev. Plant Biol. 61 (2010) 317–347. https://doi.org/10.1146/annurev-arplant-042809-112119.

[21] W. Wilms, M. Woźniak-Karczewska, A. Syguda, M. Niemczak, Ł. Ławniczak, J. Pernak, R.D. Rogers, Ł. Chrzanowski, Herbicidal Ionic Liquids: A Promising Future for Old Herbicides? Review on Synthesis, Toxicity, Biodegradation, and Efficacy Studies, J. Agric. Food Chem. 68 (2020) 10456–10488. https://doi.org/10.1021/acs.jafc.0c02894.

[22] W. Stachowiak, M. Smolibowski, D.K. Kaczmarek, T. Rzemieniecki, M. Niemczak, Toward revealing the role of the cation in the phytotoxicity of the betaine-based esterquats comprising dicamba herbicide, Sci. Total Environ. 845 (2022) 157181.

https://doi.org/10.1016/j.scitotenv.2022.157181.

[23] W. Stachowiak, D.K. Kaczmarek, T. Rzemieniecki, M. Niemczak, Sustainable Design of New Ionic Forms of Vitamin B3 and Their Utilization as Plant Protection Agents, J. Agric. Food Chem. 70 (2022) 8222–8232. https://doi.org/10.1021/acs.jafc.2c01807.

[24] F. Menges, Spectragryph - optical spectroscopy software, (2009). http://www.effemm2.de/spectragryph/.

[25] M. Niemczak, T. Rzemieniecki, A. Biedziak, K. Marcinkowska, J. Pernak, Synthesis and Structure–Property Relationships in Herbicidal Ionic Liquids and their Double Salts, Chempluschem 83 (2018). https://doi.org/10.1002/cplu.201800251.

[26] T. Rzemieniecki, M. Wojcieszak, K. Materna, T. Praczyk, J. Pernak, Synthetic auxin-based double salt ionic liquids as herbicides with improved physicochemical properties and biological activity, J. Mol. Liq. (2021) 116452. https://doi.org/10.1016/j.molliq.2021.116452.

[27] A.H. Rahim, N.M. Yunus, W.S. Hamzah, A. Sarwono, N. Muhammad, Low-Viscosity Ether-Functionalized Ionic Liquids as Solvents for the Enhancement of Lignocellulosic Biomass Dissolution, Processes 9 (2021). https://doi.org/10.3390/pr9020261.

[28] A.S.L. Gouveia, L.C. Tomé, I.M. Marrucho, Density, Viscosity, and Refractive Index of Ionic Liquid Mixtures Containing Cyano and Amino Acid-Based Anions, J. Chem. Eng. Data 61 (2016) 83–93. https://doi.org/10.1021/acs.jced.5b00242.

[29] OECD, Test No. 201: Freshwater Alga and Cyanobacteria, Growth Inhibition Test, 2011. https://doi.org/10.1787/9789264069923-en.

[30] D. Prat, A. Wells, J. Hayler, H. Sneddon, C.R. McElroy, S. Abou-Shehada, P.J. Dunn, CHEM21 selection guide of classical- and less classical-solvents, Green Chem. 18 (2016) 288–296. https://doi.org/10.1039/C5GC01008J.

[31] J. Jacquemin, P. Husson, A.A.H. Padua, V. Majer, Density and viscosity of several pure and water-saturated ionic liquids, Green Chem. 8 (2006) 172–180. https://doi.org/10.1039/B513231B.

[32] B. Yoo, W. Afzal, J.M. Prausnitz, Effect of Water on the Densities and Viscosities of Some Ionic Liquids Containing a Phosphonium Cation, 227 (2013) 157–166. https://doi.org/10.1524/zpch.2013.0328.

[33] K. Kaneko, Y. Yoshimura, A. Shimizu, Water concentration dependence of the refractive index of various ionic liquid-water mixtures, J. Mol. Liq. 250 (2018) 283–286. https://doi.org/10.1016/j.molliq.2017.12.009.

[34] M. Brüssel, M. Brehm, A.S. Pensado, F. Malberg, M. Ramzan, A. Stark, B. Kirchner,

29

On the ideality of binary mixtures of ionic liquids, Phys. Chem. Chem. Phys. 14 (2012) 13204–13215. https://doi.org/10.1039/C2CP41926B.

[35] D. Lengvinaitė, S. Kvedaraviciute, S. Bielskutė, V. Klimavicius, V. Balevicius, F. Mocci, A. Laaksonen, K. Aidas, Structural Features of the [C4mim][Cl] Ionic Liquid and Its Mixtures with Water: Insight from a 1H NMR Experimental and QM/MD Study, J. Phys. Chem. B 125 (2021) 13255–13266. https://doi.org/10.1021/acs.jpcb.1c08215.

[36] S. Marullo, F. D'Anna, P.R. Campodonico, R. Noto, Ionic liquid binary mixtures: how different factors contribute to determine their effect on the reactivity, RSC Adv. 6 (2016) 90165–90171. https://doi.org/10.1039/C6RA12836J.

[37] F. D'Anna, S. Marullo, P. Vitale, R. Noto, Binary Mixtures of Ionic Liquids: A Joint Approach to Investigate their Properties and Catalytic Ability, ChemPhysChem 13 (2012) 1877–1884. https://doi.org/10.1002/cphc.201100878.

[38] M. Niemczak, T. Rzemieniecki, D.K. Kaczmarek, A. Olejniczak, W. Stachowiak, Does the method of combining individual components affect the structure of heteroconjugated oligomeric ionic liquids?, J. Mol. Liq. 393 (2024) 123608. https://doi.org/10.1016/j.molliq.2023.123608.

[39] M. Montanino, M. Moreno, F. Alessandrini, G.B. Appetecchi, S. Passerini, Q. Zhou, W.A. Henderson, Physical and electrochemical properties of binary ionic liquid mixtures: (1−x) PYR14TFSI–(x) PYR14IM14, Electrochim. Acta 60 (2012) 163–169. https://doi.org/10.1016/j.electacta.2011.11.030.

[40] C.Z. Tan, Dependence of the refractive index on density, temperature, and the wavelength of the incident light, Eur. Phys. J. B 94 (2021) 139. https://doi.org/10.1140/epjb/s10051-021-00147-2.

[41] Z. Wang, C. Dai, J. Liu, Y. Dong, J. Liu, N. Sun, L. Li, Anionic-nonionic and nonionic mixed surfactant systems for oil displacement: Impact of ethoxylate chain lengths on the synergistic effect, Colloids Surfaces A Physicochem. Eng. Asp. 678 (2023) 132436. https://doi.org/10.1016/j.colsurfa.2023.132436.

[42] C. La Mesa, G. Risuleo, Surface Activity and Efficiency of Cat-Anionic Surfactant Mixtures, Front. Chem. 9 (2021). https://doi.org/10.3389/fchem.2021.790873.

[43] J.H. Clint, Micellization of mixed nonionic surface active agents, J. Chem. Soc. Faraday Trans. 1 Phys. Chem. Condens. Phases 71 (1975) 1327–1334. https://doi.org/10.1039/F19757101327.

[44] L.-S. Hao, Y.-F. Jia, Q. Liu, Y. Wang, G.-Y. Xu, Y.-Q. Nan, Influences of molecular

structure of the cationic surfactant, additives and medium on the micellization of cationic/anionic surfactant mixed systems, Colloids Surfaces A Physicochem. Eng. Asp. 511 (2016) 91–104. https://doi.org/10.1016/j.colsurfa.2016.09.054.

[45] M. Bergström, J.C. Eriksson, Synergistic effects in binary surfactant mixtures BT - Trends in Colloid and Interface Science XVI, in: M. Miguel, H.D. Burrows (Eds.), Springer Berlin Heidelberg, Berlin, Heidelberg, 2004: pp. 16–22.

[46] A.Z. Naqvi, S. Noori, Kabir-ud-Din, Effect of surfactant structure on the mixed micelle formation of cationic gemini–zwitterionic phospholipid systems, Colloids Surfaces A Physicochem. Eng. Asp. 477 (2015) 9–18. https://doi.org/10.1016/j.colsurfa.2015.03.009.

[47] D. Szymaniak, A. Maćkowiak, K. Ciarka, T. Praczyk, K. Marcinkowska, J. Pernak, Synthesis and Characterization of Double-Salt Herbicidal Ionic Liquids Comprising both 4-Chloro-2-methylphenoxyacetate and trans-Cinnamate Anions, Chempluschem 85 (2020) 2281–2289. https://doi.org/10.1002/cplu.202000546.

[48] E.G. Lemraski, Z. pouyanfar, Prediction of surface tension, surface mole fraction and thickness of the surface layer in the ionic liquid binary mixtures, J. Mol. Liq. 203 (2015) 52–58. https://doi.org/10.1016/j.molliq.2014.12.030.

[49] D.K. Kaczmarek, T. Rzemieniecki, D. Gwiazdowska, T. Kleiber, T. Praczyk, J. Pernak, Choline-based ionic liquids as adjuvants in pesticide formulation, J. Mol. Liq. 327 (2021) 114792. https://doi.org/10.1016/j.molliq.2020.114792.

[50] B. Jańczuk, T. Białopiotrowicz, A. Zdziennicka, Some Remarks on the Components of the Liquid Surface Free Energy, J. Colloid Interface Sci. 211 (1999) 96–103. https://doi.org/10.1006/jcis.1998.5990.

[51] A. Zajac, R. Kukawka, A. Pawlowska-Zygarowicz, O. Stolarska, M. Smiglak, Ionic liquids as bioactive chemical tools for use in agriculture and the preservation of agricultural products, Green Chem. 20 (2018) 4764–4789. https://doi.org/10.1039/C8GC01424H.

[52] Y. Chen, M. Geurts, S.B. Sjollema, N.I. Kramer, J.L.M. Hermens, S.T.J. Droge, Acute toxicity of the cationic surfactant C12-benzalkonium in different bioassays: How test design affects bioavailability and effect concentrations, Environ. Toxicol. Chem. 33 (2014) 606–615. https://doi.org/10.1002/etc.2465.

[53] M. Zhu, F. Ge, R. Zhu, X. Wang, X. Zheng, A DFT-based QSAR study of the toxicity of quaternary ammonium compounds on Chlorella vulgaris, Chemosphere 80 (2010) 46–52. https://doi.org/10.1016/j.chemosphere.2010.03.044.

[54] V. Calatrava, E.F.Y. Hom, Q. Guan, A. Llamas, E. Fernández, A. Galván, Genetic evidence for algal auxin production in Chlamydomonas and its role in algal-bacterial mutualism, IScience 27 (2024). https://doi.org/10.1016/j.isci.2023.108762.

[55] A. Piotrowska-Niczyporuk, A. Bajguz, The effect of natural and synthetic auxins on the growth, metabolite content and antioxidant response of green alga Chlorella vulgaris (Trebouxiophyceae), Plant Growth Regul. 73 (2014) 57–66. https://doi.org/10.1007/s10725-013-9867-7.

[56] P.A. Morton, C. Fennell, R. Cassidy, D. Doody, O. Fenton, P.-E. Mellander, P. Jordan, A review of the pesticide MCPA in the land-water environment and emerging research needs, WIREs Water 7 (2020) e1402. https://doi.org/10.1002/wat2.1402.

[57] G. Jing, Z. Zhou, J. Zhuo, Quantitative structure–activity relationship (QSAR) study of toxicity of quaternary ammonium compounds on Chlorella pyrenoidosa and Scenedesmus quadricauda, Chemosphere 86 (2012) 76–82. https://doi.org/10.1016/j.chemosphere.2011.09.021.

[58] M.J. Rosen, F. Li, S.W. Morrall, D.J. Versteeg, The Relationship between the Interfacial Properties of Surfactants and Their Toxicity to Aquatic Organisms, Environ. Sci. Technol. 35 (2001) 954–959. https://doi.org/10.1021/es0015141.

[59] S.E. Watson, C.H. Taylor, V. Bell, T.R. Bellamy, A.S. Hooper, H. Taylor, M. Jouault, P. Kille, R.G. Perkins, Impact of copper sulphate treatment on cyanobacterial blooms and subsequent water quality risks, J. Environ. Manage. 366 (2024) 121828. https://doi.org/10.1016/j.jenvman.2024.121828.